JOURNAL OF GEOPHYSICAL RESEARCH, VOL. 111, G02015, doi:10.1029/2005JG000135, 2006

Landscape estimation of canopy C:N ratios under variable drought stress in Northern Great Plains rangelands

Rebecca L. Phillips,[1] Ofer Beeri,[2] and Mark Liebig[1]

Received 12 November 2005; revised 22 February 2006; accepted 9 March 2006; published 10 June 2006.

[1] Plant carbon/nitrogen ratio (C:N) exerts significant control over net primary production (NPP) for most biomes, yet remote quantification at ecosystem scales is often hindered by coarse spatial resolution and by the influence of variable plant water content on spectral absorption. Consequently, remote sensing–based estimates for ecosystem properties can be masked by hectare-scale landscape patchiness and by drought stress. We approached the water content problem first by identifying those spectra sensitive to plant C:N but not sensitive to varying intensities of plant water stress under controlled conditions. Then we tested formulae developed at a plant scale with monocultures on mixed-grass prairie field plots several times during the growing season and derived an optimum rangeland C:N formula (RCNF). The RCNF was evaluated on pastures under experimental grazing treatments using mid-resolution, multispectral sensors. Delineation of canopy C:N within and between pastures was achieved under variable canopy moisture conditions using either Landsat 5 or ASTER spectral data. Landsat 5 canopy C:N ratios were estimated four times during the 2004 growing season with <14% error (RMSE = 3.1). Estimates tracked field measurements, with greater C:N ratios in April (between 30 and 34) and lower C:N in September (between 24 and 27). We also tested the RCNF on ASTER satellite data on experimental grazing treatments and found ASTER estimates were within 9.6% of field measurements (RSME = 1.5). Spatial and temporal variability among grazing treatments and collections times were similar to remote estimates despite variable plant moisture, indicating that rangeland C:N may be quantified using current, economical, satellite sensors within ±3 C:N units.

Citation: Phillips, R. L., O. Beeri, and M. Liebig (2006), Landscape estimation of canopy C:N ratios under variable drought stress in Northern Great Plains rangelands, *J. Geophys. Res.*, *111*, G02015, doi:10.1029/2005JG000135.

1. Introduction

[2] Carbon/nitrogen ratio (C:N) drives terrestrial biogeochemical processes, such as decomposition and mineralization [*Murphy et al.*, 2002], and as such can strongly influence soil organic matter concentrations, C and N pool, and turnover rates [*Kelly et al.*, 2000; *Schimel et al.*, 1996, 1997; *Throop et al.*, 2004]. Leaf C:N ratio is also a highly sensitive input parameter to net primary production (NPP) models, such as the BIOME-BGC terrestrial ecosystem model [*White et al.*, 2000]. The relationship between leaf N and photosynthetic assimilation capacity has been well documented across a spectrum of climates [*Wright et al.*, 2004], which can be approximated from C:N ratio for a specific ecosystem. From a regional, rangeland management perspective, C:N ratio is an indicator of vegetation quality during the growing season and litter quality at senescence. Consequently, C:N represents a measurable landscape-scale signal of vegetation quality that, if remotely derived from satellite data, could improve regional NPP and rangeland quality assessment models by providing real-time C:N values at ecosystem scales. Further, by employing multispectral satellite data, input from archived imagery would be available for retrospective NPP analyses, and for identification of precursors to climate change [*Waring et al.*, 1986], such as nutrient stress [*Schimel et al.*, 1990]. For Northern Great Plains rangelands, sensors capable of resolving hectare-scale variability [*Hunt et al.*, 2003] are needed because plant C:N varies with management, phenology, and meteorological conditions. However, mid-resolution (<0.1 ha pixel^{-1}), satellite-based models capable of delineating measurable ecosystem properties associated with vegetation quality are lacking [*Moorhead et al.*, 1999]. We address this need for synoptic, ecologically relevant models by linking plant-to-pasture experiments to derive canopy-level C:N applicable to current, mid resolution, multispectral, sensor data.

[3] Correlations between leaf N content and spectral reflectance have been documented for hyperspectral sensors using hand-held and aerial platforms [*Mutanga and Skidmore*, 2004; *Wessman et al.*, 1988], but the reliability of such correlations under variable plant conditions

[1]Northern Great Plains Research Laboratory, USDA-ARS, Mandan, North Dakota, USA.
[2]Center for People and the Environment, University of North Dakota, Grand Forks, North Dakota, USA.

0148-0227/06/2005JG000135$09.00

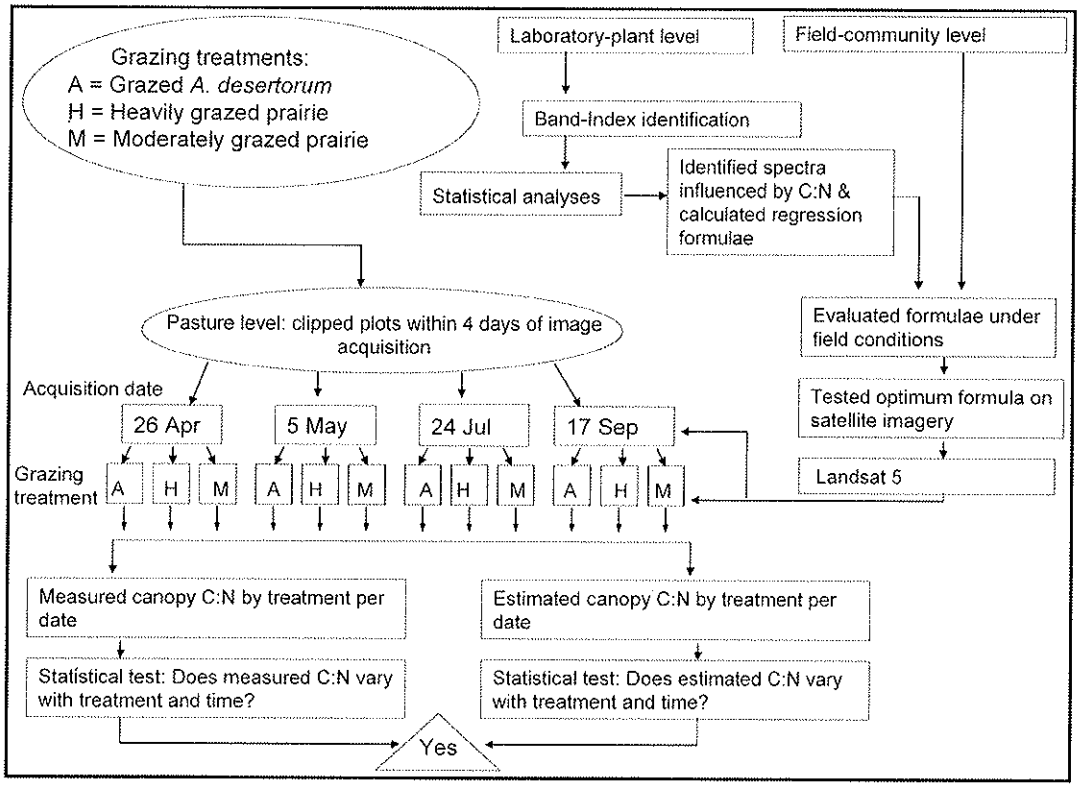

Figure 1. Outline of experimental design, from plant to pasture scales, required for spectral model development and validation.

remains uncertain. Detecting absolute plant N concentration in the field with any optical sensor presents a problem because stress associated with fluctuation in plant water content can interfere with the spectral signal [*Jacquemoud et al.*, 1996; *Kokaly and Clark*, 1999]. Hyperspectral fly-overs using aerial platforms are expensive to repeat, thereby limiting research efforts aimed toward quantifying properties that change with plant growth and meteorology. Mid-resolution multispectral satellites, such as Landsat 5 or ASTER, that regularly orbit the Earth offer more spatio-temporal options for both research and applications. We address these remote data needs by first employing a hyperspectral sensor under experimental conditions and then convolving the data to fit multispectral sensors. We address the issue of plant water content by separating the effect of water from the effect of C:N ratio on plant spectra. By experimentally testing for the effects of plant C:N and leaf water content on plant hyperspectral signatures, we developed a satellite-based C:N ratio model applicable to mixed-grass prairie rangeland under variable drought stress.

[4] We hypothesized that by separating the spectral response of leaf water content from the spectral response of leaf C:N, we could derive a formula that would estimate rangeland canopy C:N at ecologically relevant spatial and temporal scales. We chose C:N ratio because of its significance at an ecosystem scale and because the spectral signal is highly influenced by and includes information for both C and N [*Jacquemoud et al.*, 1996; *Spanner et al.*, 1985]. Consequently, we expected spectral delineation of N relative to total canopy C would be greater than for absolute N concentration [*Beeri et al.*, 2005]. Moreover, we wanted to determine those wavelengths affected by C:N for a range of plant moisture conditions under controlled conditions for a cool season (C_3) and a warm season (C_4) grass species because we intended to scale-up to Northern Plains rangeland ecosystems, where species is an important source of spectral variability [*Tieszen et al.*, 1997]. From there, we proceeded to test results from the controlled study on mixed-grass prairie using hyperspectral, plot-scale data. Then we validated the most predictive spectral model between April and September using two satellite sensors on rangelands imposed with three grazing treatments. Finally, we examined whether our satellite-based model could accurately capture spatial (field grazing treatments) and temporal (seasonal variability) patterns by comparing C:N values from plot measurements with our satellite-based estimates (Figure 1).

2. Methods

[5] For the initial plant-level phase of this work, we grew monocultures of cool season Sandburg bluegrass (*Poa secunda* (J. Presl)) and warm season blue grama (*Bouteloua gracilis* (Willd. ex Kunth) Lag. Ex Griffiths) from seed (Wind River Seed Co., Manderson, Wyoming) under similar controlled conditions to identify those spectral bands and band combinations (indices) that were influenced by plant C:N, but not by water content. Twelve flats of each species were planted in potting soil and randomly assigned to greenhouse bench space, where plants received ambient

Table 1. Relative Spectral Indices Commonly Associated With Vegetation Stress, Vegetation Water Content, or High Productivity[a]

ID	Index Name (Usage)	Index Equation	Plant Species	Water Content	C:N Ratio
1	NDVI (productivity)	$(\lambda800 - \lambda680)/(\lambda800 + \lambda680)$	<0.0001	0.0207	0.0031
2	**SAVI_0.1 (productivity)**	$1.1 \times (\lambda800 - \lambda680)/(\lambda800 + \lambda680 + 0.1)$	**<0.0001**	**0.5010**	**0.0030**
3	**WDRVI_5 (productivity)**	$(\lambda800 - 5 \times \lambda680)/(\lambda800 + 5 \times \lambda680)$	**<0.0001**	**0.0740**	**0.0030**
4	**EVI (productivity)**	$2.5 \times (\lambda800 - \lambda680)/(\lambda800 + 6 \times \lambda680 - 7.5 \times \lambda485 + 1)$	**<0.0001**	**0.4810**	**0.0040**
5	ND45 (productivity)	$(\lambda800 - \lambda1675)/(\lambda800 + \lambda1675)$	<0.0001	0.0047	0.0569
6	ND47 (productivity)	$(\lambda800 - \lambda2220)/(\lambda800 + \lambda2220)$	<0.0001	<0.0001	0.0380
7	**TC234 (productivity)**	$\lambda800 \times (\lambda555/\lambda680)$	**<0.0001**	**0.6506**	**0.0021**
8	**TC235 (productivity)**	$\lambda1675 \times (\lambda555/\lambda680)$	**<0.0001**	**0.2377**	**0.0009**
9	ND23 (productivity)	$(\lambda555 - \lambda680)/(\lambda555 + \lambda680)$	<0.0001	0.0256	<0.0001
10	**7-band GVI (productivity)**	$0.72 + \lambda1675 \times 0.07 + \lambda2220 \times -0.16 + \lambda485 \times -0.27 + \lambda555 \times -0.22 + \lambda680 \times -0.55 + \lambda800$	**<0.0001**	**0.9090**	**0.0270**
11	**ND53 (vegetation stress)**	$1 - (\lambda1675 - \lambda680)/(\lambda1675 + \lambda680)$	**<0.0001**	**0.3360**	**0.0060**
12	**ND73 (vegetation stress)**	$1 - (\lambda2220 - \lambda680)/(\lambda2220 + \lambda680)$	**0.0002**	**0.1000**	**0.0300**
13	ND52 (vegetation stress)	$(\lambda1675 - \lambda555)/(\lambda1675 + \lambda555)$	0.1984	0.0239	0.0008
14	7-band wetness (moisture)	$\lambda485 \times 0.14 + \lambda555 \times 0.18 + \lambda680 \times 0.33 + \lambda800 \times 0.34 + \lambda1675 \times -0.62 + \lambda2220 \times -0.42$	0.9050	<0.0001	0.7876
15	SR71 (moisture)	$\lambda2220/\lambda485$	0.0018	0.0364	0.0623
16	**SR31**	$\lambda640/\lambda485$	**0.0220**	**0.3870**	**0.0010**
17	**SR31**	$\lambda680/\lambda485$	**0.0090**	**0.8240**	**<0.0001**
18	**SR700/485**	$\lambda700/\lambda485$	**<0.0001**	**0.0680**	**0.0030**
19	**ND(640–680)**	$1 - (\lambda640 - \lambda680)/(\lambda640 + \lambda680)$	**0.0003**	**0.3740**	**<0.0001**

[a]Algorithms listed are results from statistical tests for the effect of plant species, water content, and C:N ratio on each index. Wavelengths (in nm) are symbolized by λ. Those given in boldface were significantly affected by C:N ratio but not significantly affected by water content. P values indicating effects of plant species, water content, and C:N ratio on spectra are listed.

sunlight conditions and air temperature ranged from 18° to 30°C. Soil moisture remained near field capacity until grasses had reached full cover, but prior to flowering, 55 days after planting. To induce progressive moisture stress, we ceased watering plants for 3 weeks following canopy closure. Spectral radiance (W m^{-2} str^{-1} nm^{-1}) was recorded between 55 and 75 days after planting for each flat using a hand-held hyperspectral spectroradiometer Field-Spec Pro (Analytical Spectral Devices Inc., Boulder, Colorado). Spectra were recorded over a full leaf canopy (~8 cm height) for a 6.6-cm diameter target area every 48 hours. To achieve a consistent and uniform target area (given the sensor 25° field of view), an aluminum arm was constructed to hold the recording gun at a fixed distance of 15 cm above the plant canopy. The hand-held receiver remained at a constant height and recorded 10 files within the target area to obtain an average. Prior to recording spectra for a target, calibration panel (Spectralon Labsphere Inc., North Sutton, New Hampshire) radiance was recorded. Reflectance (R) for each wavelength (λ) was calculated using two calibration (C) and ten target (T) records (W m^{-2} str^{-1} nm^{-1}) according to

$$R_\lambda = \left[\left(\sum_1^{10} T_\lambda\right)/10\right] / \left[\left(\sum_1^{2} C_\lambda\right)/2\right]. \quad (1)$$

We prevented interference from diffuse light by shielding targets from direct sunlight during the measurement period (between 1400 and 1600 hr) and applying a stable, controlled, 15W halogen light source (ASD Pro-Lamp) set on focused mode and oriented 15° from nadir (or 75° above the horizon). This method minimized radiance differences between flats and days that could be attributed to irradiance variability. Immediately following spectral measurements, all aboveground plant material inside the 6.6-cm target was destructively sampled. Most aboveground material was leaf, rather than stem biomass. Plant material was weighed on a microbalance and oven-dried at 60°C for 48 hours. After recording dry weights, all plant material was ground completely by hand using a mortar and pestle. All samples were analyzed for total C and N by dry combustion using a LECO CN analyzer (LECO Corp, St. Joseph, Michigan). Plant biomass, water content (g H_20 g^{-1} fresh mass), C (g C g^{-1} dry mass), and N (g N g^{-1} dry mass) were recorded for each 6.6 cm target on each date.

[6] We summarized the hyperspectral data for both species and determined wavelengths (λ) that responded linearly to an increase in plant C:N ratio. Correlation analyses were performed using all spectral records against plant C:N ratio. Spectral regions most highly correlated with C:N ratios were found in the red, blue, and midinfrared portions of the spectra. Ratios and normalized difference ratios were constructed using those wavelengths correlated with plant C:N. Most wavelengths selected were applicable to multispectral sensors satellite platforms (e.g., Landsat 5, ASTER, SPOT, MODIS). We also included common vegetation indices previously reported in the literature, such as the Normalized Difference Vegetation Index (NDVI) and the Enhanced Vegetation Index (EVI).

[7] We ran a separate analysis of variance for each of the indices as recorded by the spectroradiometer to determine effects of plant species, C:N, and water content (independent variables) on index spectral response using the SAS General Linear Models (GLM) routine (v. 8). We were interested in identifying those indices significantly affected by C:N and not by plant water content, given that plant species would also influence spectra. This three-way analysis of variance reduced the number of potential spectral algorithms for C:N detection from 19 to 12 (boldface in Table 1). For each of the remaining 12, we used regression analyses to construct a set of 24 linear and quadratic equations to serve as candidate formulae for predicting C:N in the subsequent plot-scale phase of our study. These were evaluated visually by plotting predicted values versus residuals to ensure homogeneity of regression variance.

[8] We proceeded to the plot-scale phase by testing these formulae in working rangelands. We conducted hyperspectral ground surveys for rangelands located at the USDA-ARS Northern Great Plains Research Laboratory (NGPRL) in Mandan, North Dakota, three times during the growing season (24 June, 2 August, and 23 August 2004). We collected plot-scale data from three grazing treatments; a moderately grazed (2.6 ha steer^{-1}) mixed-grass prairie, a heavily grazed (0.9 ha steer^{-1}) mixed-grass prairie, and an annually fertilized (45 kg N ha^{-1}), heavily grazed (0.9 ha steer^{-1}) field of crested wheatgrass (*Agropyron desertorum* (Fisch. ex. Link) Schult.) interseeded with *B. gracilis* [*Liebig et al.*, 2006]. Spectral reflectance (nadir) was recorded at 1100 hr 1.5 m above the canopy in four 1-m^2 plots selected at random within each treatment on each date. Directly after spectra were recorded, standing biomass and litter was harvested using 0.25 m^2 quadrats and material was separated into litter, standing-dead, and standing-live material. Carbon and N concentrations for each pool (standing-live, standing-dead, and litter) were determined by dry combustion and the weighted mean calculated to include all plant material for canopy C:N. The high contribution of standing-dead and litter to aboveground biomass in the field necessitated inclusion of these pools, since rangeland pixels include a mix of plant live and dead materials, including detritus.

[9] Plot-scale data collected 24 June, 2 August, and 23 August (ground-truth hyperspectral and canopy C:N) were used to evaluate the 24 linear and quadratic candidate formulae constructed from the greenhouse phase of our study (boldface in Table 1) by plotting predicted C:N against measured C:N for these dates. The best predictor of field-plot C:N ratio was then evaluated intraseasonally using multispectral satellite data for pastures at the NGPRL. Plot-scale data variability was evaluated for homoscedasticity using this index equation by convolving hyperspectral data to multispectral bands for observations recorded 2 August.

[10] For the multispectral, landscape-scale phase of our study, we acquired four cloud-free Landsat 5 scenes and one cloud-free ASTER scene during the 2004 growing season. We used ERDAS Imagine 8.7 (Leica Geosystems GIS & Mapping LLC.) to geo-reference and calibrate each image to UTM, Zone 14 projection and WGS 84 Datum with ground-control points. Ten geo-locations were mapped using a Trimble Geo XT Geographic Position System (GPS) Beacon receiver with an external antenna to achieve submeter locational accuracy. We converted the Landsat 5 pixel digital numbers to ground reflectance by using MODTRAN-4 radiative transfer code inside the ATCOR 2 package [*Geosystems*, 2002] and the specific calibration files for each band [*Chandler and Markham*, 2003]. The ASTER digital numbers were converted to ground reflectance using the empirical line method [*Clark et al.*, 2002; *Geosystems*, 2002; *Moran et al.*, 2001].

[11] Model validation was performed with field observations for all pasture treatments five times during the growing season in conjunction with satellite flyovers. Four 0.25-m^2 plots were clipped to ground level within each pasture and standing-live, standing-dead, and litter material separated, weighed and analyzed for C and N as described above within four (Landsat 5) or six (ASTER) days of satellite overpass. Landsat 5 imagery was acquired 26 April, 5 May, 24 July, and 17 September, while ASTER was acquired 20 May. Canopy C:N was estimated using satellite image data and the C:N model for 12 pixels inside each image. Root mean square error (RMSE) and relative error (RE) were calculated for each pixel (estimated) against measurements inside each pixel (actual) and the absolute values summed and divided by the total number of pixels for each sensor separately.

$$RMSE = \sqrt{\left\{\left[\sum_1^n (Actual - Estimated)^2\right]/n\right\}} \quad (2)$$

$$RE = \left\{\sum_1^n [(Actual - Estimated)/Actual]\right\}/n, \quad (3)$$

where "Actual" represent the ground measurements and *estimated* represent the satellite estimates.

[12] We analyzed Landsat 5-estimated C:N, ASTER-estimated C:N, and measured canopy C:N separately from each other owing to differences in sampling and pixel spatial scales. The fixed effects of grazing treatment and time on plot-scale (0.25 m^2) and on Landsat 5 pixel-scale (900 m^2) C:N ratio were tested using a repeated measures, mixed model (SAS Inc., Cary, North Carolina) with random effects of plot nested inside treatment for each of the satellite flyover dates [*Littell et al.*, 1996]. Since the time $\times$ treat interaction was not significant, it was excluded from both models. The fixed effects of grazing treatment on plot-scale and on ASTER pixel-scale (225 m^2) C:N ratios were tested separately using a mixed model with random effects of plot nested inside treatment. For analyzing effects of grazing treatment and time on plant canopy moisture content, standing-dead mass, standing-live mass, and litter mass we used data for all eight field observations (26 April, 5 May, 24 June, 24 July, 2 August, 23 August, and 17 September).

3. Results

[13] Withholding water from *Poa secunda* in the greenhouse experiment resulted in greater water stress than for *Bouteloua gracilis*. Initial water content for *P. secunda* was 80% and fell to 30%, while the 77% initial water content for *B. gracilis* fell to 40%. C:N values for *P. secunda* ranged from 10 to 36, while *B. gracilis* C:N ranged from 19 to 61. Aboveground biomass for both species was similar. Averaged across all sample dates, biomass was estimated at 101 g m^{-2} for *P. secunda* and 120 g m^{-2} for *B. gracilis*. Each candidate index was quantitatively evaluated for effects of water content on spectra, which was significant for 12 of the 19 index equations tested (Table 1). A significant portion of statistical variance was also attributed to differences between *P. secunda* and *B. gracilis* species, likely due to morphological differences (color, architecture, structure) between the two grasses. Six multispectral productivity indices, two multispectral vegetation stress indices, three multispectral simple ratio indices, and one hyperspectral index were included in the list of 12 indices significantly affected by C:N ratio and species but not affected by water content (boldface in Table 1).

Table 2. Mean and Standard Deviation for 0.25 m^2 Clipped Field Plots by Date and by Grazing Treatment[a]

		Standing-Live, kg ha^{-1}		Standing-Dead, kg ha^{-1}		Fraction Standing-Dead		Litter, kg ha^{-1}	
Date	Treat	Mean	Std Dev	Mean	Std Dev	Mean	Std Dev	Mean	Std Dev
26 April	A	452	243	729	305	0.62	0.13	819	416
	H	165	59	584	125	0.78	0.06	241	136
	M	252	87	2474	442	0.91	0.03	1729	509
10 May	A	618	199	963	193	0.61	0.09	549	323
	H	540	116	1180	480	0.68	0.05	180	116
	M	407	152	3256	239	0.89	0.04	927	381
26 May	A	667	225	1181	360	0.63	0.11	871	411
	H	633	205	703	377	0.50	0.18	142	128
	M	614	187	2610	827	0.80	0.09	2241	933
21 June	A	610	202	875	150	0.60	0.05	751	301
	H	602	141	514	327	0.44	0.19	323	54
	M	735	100	1657	544	0.68	0.07	1900	279
20 July	A	566	153	437	154	0.43	0.14	949	273
	H	702	60	554	287	0.42	0.14	235	97
	M	816	212	2865	446	0.78	0.06	2360	638
2 Aug	A	464	54	591	211	0.55	0.10	1300	438
	H	644	207	734	604	0.49	0.21	790	346
	M	978	203	1259	389	0.56	0.04	3141	1150
23 Aug	A	356	50	772	328	0.67	0.11	890	517
	H	365	98	548	177	0.60	0.08	285	172
	M	745	157	2792	1151	0.78	0.05	1705	315
20 Sep	A	547	167	625	266	0.53	0.08	706	478
	H	281	209	526	249	0.65	0.19	370	377
	M	751	194	1390	263	0.65	0.05	1867	480

[a]Plots clipped to ground level were separated into standing-live and standing-dead pools. Remaining material on the ground was collected as litter. Treatment A is heavily grazed *A. desertorum*, treatment H is heavily grazed mixed-grass, and treatment M is moderately grazed mixed-grass (see text for details).

[14] The regression formulae derived for each index based on observations collected in the greenhouse were then tested on field plots located inside grazing treatments. Most formulae, when applied to hyperspectral records collected from grassland communities, did not agree well with field measurements (predicted vs. measured regressions were not significant, with R^2 values < 0.5). This was particularly apparent for those formula requiring blue and green regions of the spectra. We suspect this is likely due to interference from the exceptionally high proportion of litter and standing-dead material to total canopy mass. Each of these pools consistently contributed more to total biomass than live material in these rangelands during 2004. Under field conditions, the best estimate for C:N was achieved from the ND53 (Table 1), which utilizes 680 and 1675 nm wavelengths. These bands are similar to Landsat 5 and ASTER spectral responses for red and midinfrared (IR) bands. Spectral response for other satellite sensors, such as SPOT and MODIS, require a shift in wave band values, specifically 645 and 1610 nm, and 645 and 1630 nm, respectively [*Beeri et al.*, 2005]. These SPOT- and MODIS-specific indices (12, 13 and 15 in Table 1) were not significantly related to plant C:N, contrary to wave bands available from Landsat 5 and ASTER sensors. The specific range required for C:N delineation suggests that satellite detection of plant C:N may be sensor specific.

[15] Of the 24 formulae derived from the greenhouse phase of our study, linear (equation (4)) and quadratic (equation (5)) equations applying the ND53 index (Table 1) were the best predictors of canopy C:N at the field-plot scale.

$$C:N = 2.62 + 56.35 * \left[1 - \left(\frac{\lambda 1675 - \lambda 680}{\lambda 1675 + \lambda 680}\right)\right] \quad (4)$$

$$C:N = 63.4 - 219.7 * \left[1 - \left(\frac{\lambda 1675 - \lambda 680}{\lambda 1675 + \lambda 680}\right)\right] + 305.0 * \left[1 - \left(\frac{\lambda 1675 - \lambda 680}{\lambda 1675 + \lambda 680}\right)\right]^2, \quad (5)$$

where data inputs at specific wavelengths are symbolized by λ. We found equation (5) to provide the best fit to ground data and utilized the quadratic formula for subsequent procedures and refer to this equation as the Range C:N Formula (RCNF). Hyperspectral data collected at the plot scale on 2 August were similar among treatments, with average (± standard deviation) index values of 0.45 ± 0.13 for fertilized range, 0.46 ± 0.18 for heavily grazed range, and 0.47 ± 0.17 for moderately grazed range.

[16] The mass of standing-dead material varied with grazing treatment ($df = 2, 9$; $F = 84.97$ $p < 0.001$) and with time ($df = 1, 83$; $F = 10.90$ $p < 0.001$). The fraction of standing-dead for all grazing treatments was greatest in April and declined until August, when the proportion of standing-dead began to rise again (Table 2). Standing-dead material was greatest for moderately grazed range at all collection times. Averaged across dates, standing-dead material for fertilized and unfertilized heavily grazed range was 772 and 668 kg ha^{-1}, respectively, while the moderately grazed range was 2288 kg ha^{-1}.

[17] Similar to standing-dead, litter mass was also significantly affected by grazing treatment ($df = 2, 9$; $F = 32.42$ $p < 0.001$) and time ($df = 1, 83$; $F = 5.52$ $p < 0.021$), with consistently greater litter in the moderately grazed plots throughout the season. Differences among treatments for the litter pool were greater than for the standing-dead pool, with fertilized range at 854 kg ha^{-1}, unfertilized, heavily grazed

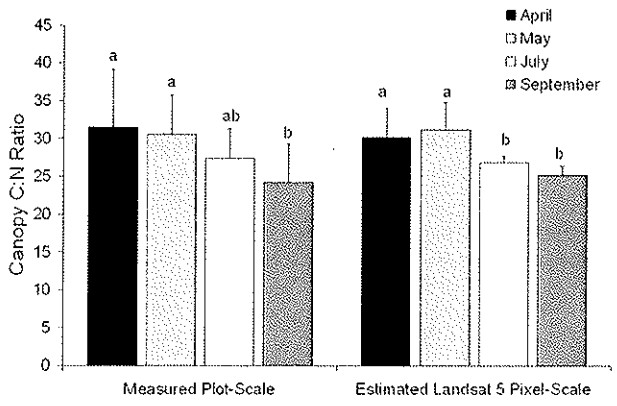

Figure 2. Mean (±std. dev.) canopy C:N measured from field plots by date. Plot data were collected with 3 days of image acquisition at four times during the growing season 2004 next to estimated, Landsat 5 pixel-scale mean (±std dev) canopy C:N. Letters over error bars denote significant differences for measured and estimated C:N with time.

range at 321 kg ha^{-1}, and unfertilized, moderately grazed range at 1984 kg ha^{-1}. Unlike standing-dead material, highest values were recorded during the mid-summer months.

[18] For standing-live material, the effect of treatment varied intraseasonally (time × treatment df = 2, 81 F = 9.06 $p < 0.001$). Live material in the fertilized, heavily grazed *A. desertorum* peaked more quickly and to a lesser degree than the moderately grazed mixed-grass prairie, where standing-live material maximum was recorded 2 August at 978 kg ha^{-1}. Fertilized, heavily grazed range maximum was recorded 26 May at 667 kg ha^{-1}. Heavily grazed mixed-grass range was intermediate between these treatments with maximum recorded 20 July at 702 kg ha^{-1}.

[19] Plant canopy moisture content (both standing-live and standing-dead material) varied with collection date (df = 1, 47; F = 9.32, $p < 0.0037$) and with grazing treatment (df = 2, 9; F = 5.78 $p < 0.0243$) between April and September. Moisture content for heavily grazed and fertilized *A. desertorum* was consistently higher than moderately grazed and heavily grazed mixed-grass pastures. Canopy moisture was greatest in September (66, 54, and 58%, respectively, for A, M, and H treatments) and lowest in August (49, 42, and 36%, respectively, for A, M, and H treatments). Overall mean canopy moisture for all collection five dates was 52% for *A. desertorum*, 43% moderately grazed, and 41% for heavily grazed mixed-grass range.

[20] The effects of grazing treatment and collection time on measured C:N for sample collection dates were analyzed separately from Landsat 5 and ASTER estimates because spatial resolution varied among measured C:N (0.25 m^2), Landsat 5 (900 m^2), and ASTER (225 m^2) pixels. The C:N formula is common to both the ASTER and Landsat 5 sensors because important spectral response regions within the red and mid-Infrared bands, respectively, are similar (Landsat 5, 626–693 nm versus ASTER, 628–691 nm; Landsat 5, 1570–1783 nm versus ASTER, 1609–1702 nm). We tested (1) if plot-scale C:N and Landsat 5 C:N estimates varied with grazing treatment (spatially) and time (temporally) using a two-way repeated measures analysis of variance (ANOVA), and (2) if plot-scale C:N and ASTER C:N estimates for C:N varied with grazing treatment (spatially) using a one-way ANOVA. We also used separate Bonferroni's t-test for a posteriori means comparisons among Landsat 5 estimates, ASTER estimates, and plot measurements. Heavily grazed *A. desertorum* C:N ratio was consistently lower than moderately grazed and heavily grazed mixed-grass range on each date, according to plot measurements (treatment $F_{2,9} = 19.80$ $p < 0.0005$; time $F_{1,35} = 26.93$, $p < 0.0001$) and Landsat 5 estimates (treatment $F_{2,9} = 25.53$, $p < 0.0002$; time $F_{1,35} = 73.16$, $p < 0.0001$). On 20 May, the effect of grazing treatment was evident for both plot measurements (treatment $F_{2,9} = 6.46$, $p < 0.182$) and ASTER estimates (treatment $F_{2,9} = 12.29$, $p < 0.0027$). In each case, satellite estimates tracked plot measurements with significant effects of time (Figure 2) and treatment (Figures 2 and 3). Spatial constraints are evident when comparing Landsat 5 (Figure 3a) to ASTER (Figure 3b). Resolution of plot-scale variability is more limited with Landsat 5 than ASTER, likely owing to pixel size differences, and underscores consideration of spatial scale when assessing vegetation quality across a landscape.

[21] Mean Landsat 5-based estimates for canopy C:N ratios were within ±1 C:N unit at each image acquisition date (Figure 2) despite variable canopy moisture levels. Averaged over the four dates, estimated C:N varied with grazing treatments, with lower C:N for fertilized *A. desertorum* (25.8 ± 1.4) than for heavily and moderately grazed mixed-grass prairie (28.8 ± 2.5, 30.6 ± 4.5, respectively). Estimates are in agreement with trends for measured C:N, which were lower for fertilized *A. desertorum* (23 ± 4.4) than for heavily and moderately grazed pastures (31.3 ± 4.4, 31.1 ± 5.5, respectively). Similarly, RCNF estimates for canopy C:N ratios using ASTER were in accordance with field measurements for the three grazing treatments (Figure 3), despite differences in canopy moisture content. Field validation of the multispectral model derived from the hyperspectral, plant and plot scale data, suggest that satellite delineation of C:N using the RCNF is not influenced by variable rangeland canopy moisture.

[22] The quadratic form of the equation utilizing the ND53 index (RCNF) more closely estimated C:N than the linear form for ASTER data, with lower root mean square error (RMSE), while error for Landsat 5 linear and quadratic model estimates were similar. The linear relationship between RCNF-estimated and measured mean C:N for each treatment was stronger for ASTER ($R^2 = 0.83$, n = 12) than for Landsat 5 ($R^2 = 0.69$, n = 48), although only one ASTER scene (versus four Landsat 5 scenes) was evaluated. Overall, RMSE for intraseasonal Landsat 5 estimates was 3.1 C:N units with a mean 13.8% relative error between actual and predicted values, whereas RMSE for ASTER estimates was 1.6 C:N units, with a mean 9.6% relative error.

[23] Canopy C:N differences on 20 May among moderately grazed (M), heavily grazed (H) and heavily grazed *A. desertorum* (A) enclosures, corresponding to mean values estimated by the RCNF (Figure 3), are mapped on an ASTER image (Figure 4). The bright yellow areas represent recently planted experimental plots or bare soil. The cluster of dark green pixels to the east of pasture A is cultivated alfalfa. Figure 4 is a faction of the full image (>200 km^2) that may be geospatially analyzed from pasture to regional

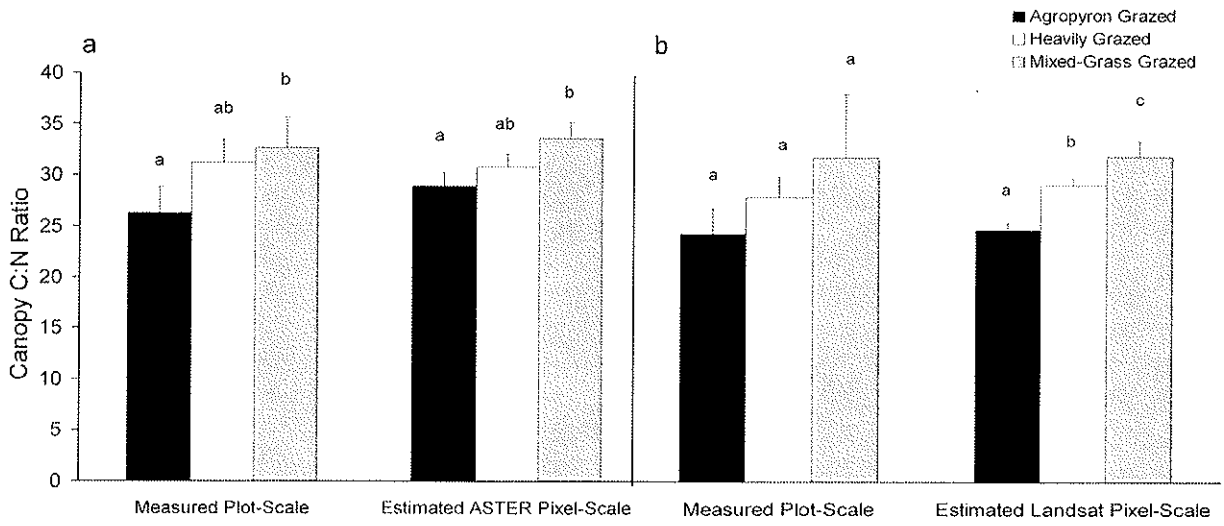

Figure 3. Mean (±std. dev.) canopy C:N measured from field plots for each grazing treatment next to (a) ASTER-estimated mean (±std. dev.) on 20 May and (b) Landsat 5 estimated mean (±std dev) on 5 May for each grazing treatment. Letters over error bars denote significant differences among treatments for plot-scale and pixel-scale canopy C:N.

scales in a geographic information systems (GIS) framework. For illustrative purposes, differences in C:N ratios among pastures are evident by shades of green and yellow. For the area just south of treatment M (hayed the previous fall), C:N is 25, in contrast with pasture M (moderately grazed) where C:N is 35. Given a 40% carbon content typical of these rangelands (data not shown), a C:N ratio of 35 equals 1.14% N or 7.14% crude protein, which is below the nutrition threshold (~8% crude protein) for most ruminants (S. Kronberg, manuscript in preparation, 2006). In this case, a 10-point difference in C:N ratio between pasture M and the pasture south of M signifies a 3% difference in crude protein, from 7.14 to 10.2%. When nutritional requirements are not met, moving animals from lower to higher quality pastures is common. These types of landscape data, especially when combined with local knowledge, provide practical management information as well as insight into factors influencing C:N under vacillating environmental conditions.

4. Discussion

[24] Grazing is known to invoke changes in rangeland community structure and vegetative quantity and quality, depending upon factors such as grazing intensity and timing of defoliation. The net effect of grazing on rangeland health will vary with phenology and weather, so remote-based tools that resolve pasture-scale variability and that are appropriate for the ecoregion are called for by managers and modelers. This work reports variable drought and grazing stress and effects on C:N while validating a new satellite model. The heavily grazed and fertilized *A. desertorum* treatment was significantly lower in canopy C:N (greater forage quality), compared with mixed-grass grazing treatments. The fertilizer "benefit" is given by a four- to ten-unit decrease in C:N, with differences between treatments narrowing with time between April and September. This may or may not lead to appreciable benefits in animal production, depending upon how close the material may be to minimum ruminant crude protein requirements.

[25] Laboratory studies have accurately determined optimum wavelengths for leaf N detection using hyperspectral sensors on dried plant material (2054 and 2172 nm), and have determined that this signal is masked by water in living tissue [*Kokaly*, 2001]. Hyperspectral research in grasslands [*Mutanga and Skidmore*, 2004] report canopy N content correlated with band combinations in the green (521 and 566 nm), far-red (747 nm), and midinfrared (1523 nm) spectral regions, but effects of varying moisture conditions remains uncertain. Here, we address the plant water issue by developing a spectral algorithm under variable drought stress and testing this algorithm in the field. Model accuracy is consistent intraseasonally under variable moisture status, which we attributed to separation spectra associated with water from C:N. Further, model evaluation steps at plot and pasture scales validated satellite application efficacy.

[26] By developing a model using two disparate grass species and testing the efficacy of the model in a mixed-grass prairie, some morphological differentiation is built into the model to better serve large-scale application needs for mixed rangeland ecosystems. Spectral investigations using monocultures elicit valuable species-specific response variables, which vary with respect to plant phenology, canopy architecture, pigmentation, structural carbohydrates, etc. In our case, we included both species, so that some of the species-specific spectral variability might be partitioned into the model separate from C:N and water content. However, we did not evaluate mixtures of rangeland species during the controlled greenhouse experiment. Instead, we used plot-scale measurements to evaluate mixed communities. Species effects may have contributed to the lack of fit between measured and modeled C:N at the plot scale for some index equations (Table 1).

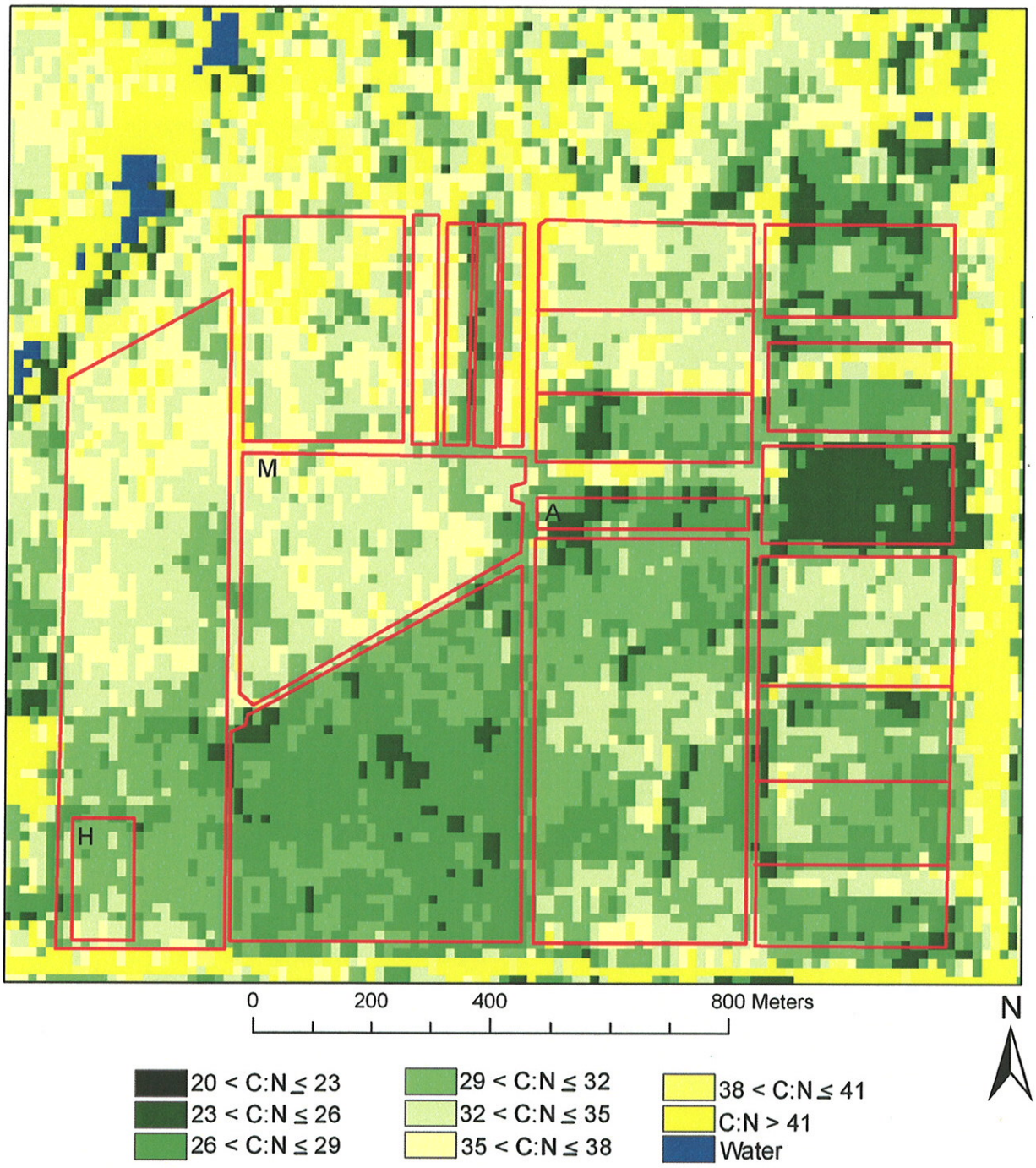

Figure 4. Location of the research site and modeled C:N ratio using ASTER data acquired 20 May. Pastures A, M, and H represent the three grazing treatments, respectively: heavily grazed *A. desertorum*, moderately grazed mixed-grass, and heavily grazed mixed-grass prairie. The surrounding enclosures represent other experimental crop and range sites grazed by cattle at varying times and intensities.

[27] We tested the RCNF on experimental pastures using intensive ground surveys of both live and dead plant material for weighted, canopy C:N delineation. Effects of grazing treatments on C:N ratios observed in the field were estimated using the RCNF model and Landsat 5 satellite imagery with <14% error. Canopy C:N decreased between April and September, according to both field measurements and satellite estimates. This may be attributed to shifts in distribution of standing-dead material between the beginning and end of the season, and/or the timing of precipitation events. Late-summer rainfall may have stimulated new growth, especially in the moderately grazed range (Table 2).

[28] Standing-dead and litter pools each contributed more to total biomass than standing-live; consequently senescent

and detrital material pools were essential to model development and testing. We aimed to include senescent material in our model because both live and senescent materials contribute carbon and nutrients to rangeland ecosystems. Moreover, estimation of C:N for senescent material is essential for plant decomposition analyses. Previous research suggests post-harvest residue mass may be estimated through application of the remote-based Cellulose Absorption Index (CAI) for wheat residue [*Streck et al.*, 2002]. Remote sensing both canopy mass and canopy quality at the end of the grazing season should improve climate-based model estimates of over-winter decomposition and nutrient turnover. Future work into spectral separation of live from standing-dead and litter materials would contribute greatly to monitoring ecosystem biogeochemistry and should be considered as a target for the next generation of satellite sensors.

[29] The RCNF was developed for rangeland vegetation and has not been tested on crop monocultures, such as small grain production, which is another common land use in this region. However, prospects for application to cropping systems is promising, in light of successes achieved with remote estimation of chlorophyll content for maize and soybean crops in Nebraska [*Gitelson et al.*, 2005]. Further validation of remote sensing models using satellite data for vegetation properties controlling ecosystem processes are needed to determine spatiotemporal accuracy of the RCNF for other agricultural ecosystems under various types of stress.

[30] C:N ratios often reflect ecosystem plasticity to environmental conditions (e.g., rainfall, herbivory, nutrient availability), expressed in changing allocation patterns, community structure, and residence times of detrital organic matter pools. Remotely derived values for vegetation C:N ratio and archived time series imagery for the mixed-grass prairie ecoregion are data potentially bridging key spatiotemporal feedback mechanisms, such as temperature, drought, fire disturbance, and grazing management, with canopy C:N responses. In conjunction with existing models, remotely derived values for vegetation C:N ratio using the RCNF should enhance research efforts aimed toward understanding multiple-scale processes on rangeland C and N cycling.

5. Conclusions

[31] We describe an integrated and innovative approach with an emphasis on bridging spatial, temporal and spectral scales for the purpose of building a satellite-based model for landscape C:N based on plant physiological data from monocultures, mixed-grass prairie field plots, and working rangelands. Results of satellite mode validation suggest the RCNF delineates rangeland canopy C:N independent of plant water stress and does so reliably in the face of seasonal variability and management treatment.

[32] For Northern Great Plains ranchers, quantification of rangeland canopy C:N with synoptic, spectral data represents a practical application of technology for use in support of grazing management decisions. Livestock producers and public land managers are calling for remote rangeland health assessment as they face increasing pressure to balance economic and conservation goals. The RCNF, which is built into a geographic information systems framework, provides the next step toward integrated management and monitoring for Northern Great Plains rangeland landscapes.

[33] For ecosystem scientists and modelers, the ability to estimate spatial and temporal patterns in rangeland C:N could enhance grassland carbon cycling models that rely on accurate inputs for NPP and litter quality [*Moorhead et al.*, 1999; *Parton et al.*, 1995; *Pastor et al.*, 1987], including BIOME-BGC [*White et al.*, 2000]. Aboveground nutrient turnover and availability relies heavily on substrate quality and weather. By specifying canopy quality in units of C:N values instead of relative reflectance units, an image acquired at the end of the growing season could be modeled to estimate, in conjunction with weather data, over-winter decomposition rates across several kilometers of rangeland. Moreover, since C:N estimates are independent of canopy moisture, climate variability within ecoregions is less likely to interfere with cross-site comparisons of vegetation quality. These steps to improve remote quantification of biogeochemically relevant properties in rangeland landscapes will scale up our understanding of terrestrial ecosystem biogeochemistry and make available the real-time data needed for assessing possible precursors to global change [*Waring et al.*, 1986], such as perturbations to ecosystem carbon and nitrogen cycles [*Hobbie*, 1996; *Schimel et al.*, 1990; *Throop et al.*, 2004].

[34] **Acknowledgments.** The authors are grateful to R. Kelman Wieder, Scott Bylin, Cory Enger, Blake Mozer, Jared Clayburn, Jason Gross, Gail Sage, and Becky Wald for their incredible contributions to this project. Special thanks to Dean Smith and Mike Poellet at the University of North Dakota John D. Odegard School of Aerospace Sciences. Thanks are owed to Wind River Seed Company for grass seed donation and to Bob Sherman from the UND Biology Department for technical support. This work was supported by USDA Cooperative Agreement 58-5445-3-314.

References

Beeri, O., R. L. Phillips, P. Carson, and M. Liebig (2005), Alternate satellite models for estimation of sugar beet residue nitrogen credit, *Agric. Ecosyst. Environ.*, *107*, 21–25.

Chandler, G., and B. Markham (2003), Revised Landsat-5 TM radiometric calibration and postcalibration dynamic ranges, *IEEE Trans. Geosci. Remote Sens.*, *41*, 2674–2677.

Clark, R. N., G. A. Swayze, K. E. Livo, R. F. Kokaly, T. V. V. King, J. B. Dalton, J. S. Vance, B. W. Rockwell, T. Hoefen, and R. R. McDougal (2002), Surface reflectance calibration of terrestrial imaging spectroscopy data: A tutorial using AVIRIS, paper presented at AVIRIS Airborne Geosciences Workshop, U.S. Geol. Surv., Pasadena, Calif. (Available at http://speclab.cr.usgs.gov/PAPERS.calibration.tutorial/)

Geosystems (2002), *ATCOR for ERDAS IMAGINE*, Riesstrasse, Germany.

Gitelson, A. A., A. Vina, C. Rundquist, V. Ciganda, and T. J. Arkebauer (2005), Remote estimation of canopy chlorophyll content in crops, *Geophys. Res. Lett.*, *32*, L08403, doi:10.1029/2005GL022688.

Hobbie, S. E. (1996), Temperature and plant species control over litter decomposition in Alaskan tundra, *Ecol. Monogr.*, *66*, 503–522.

Hunt, R. E., Jr., J. H. Everitt, J. C. Ritchie, M. S. Moran, D. T. Booth, G. L. Anderson, P. E. Clark, and M. S. Seyfried (2003), Applications and research using remote sensing for rangeland management, *Photogramm. Eng. Remote Sens.*, *69*, 675–693.

Jacquemoud, S., S. L. Ustin, J. Verdebout, G. Schmuck, G. Andreoli, and B. Hosgood (1996), Estimating leaf biochemistry using the prospect leaf optical properties model, *Remote Sens. Environ.*, *56*, 194–202.

Kelly, R. H., W. J. Parton, M. D. Hartman, L. K. Stretch, D. S. Ojima, and D. S. Schimel (2000), Intra-annual and interannual variability of ecosystem processes in shortgrass steppe, *J. Geophys. Res.*, *105*, 20,093–20,100.

Kokaly, R. F. (2001), Investigating a physical basis for spectroscopic estimates of leaf nitrogen concentration, *Remote Sens. Environ.*, *75*, 153–161.

Kokaly, R. F., and R. N. Clark (1999), Spectroscopic determination of leaf biochemistry using band depth analysis of absorption features and stepwise linear regression, *Remote Sens. Environ.*, *67*, 267–287.

Liebig, M. A., A. Frank, J. Gross, J. Hanson, S. Kronberg, and R. L. Phillips (2006), Soil response to long-term grazing in the Northern Great Plains of North America, *Agric. Ecosyst. Environ.*, *115*, 270–276.

Littell, R. C., G. A. Milliken, W. W. Stroup, and R. D. Wolfinger (1996), *SAS System for Mixed Models*, SAS Inst., Cary, N. C.

Moorhead, D. L., W. S. Currie, E. B. Rastetter, W. J. Parton, and M. E. Harmon (1999), Climate and litter quality controls on decomposition: An analysis of modeling approaches, *Global Biogeochem. Cycles*, *13*, 575–590.

Moran, M. S., R. Bryant, W. Thome, W. Ni, Y. Nouvellon, M. P. Gonzalez-Dugo, J. Qi, and T. R. Clarke (2001), A refined empirical line approach for reflectance factor retrieval from Landsat-5 TM and Landsat-7 ETM+, *Remote Sens. Environ.*, *78*, 71–82.

Murphy, K. L., I. C. Burke, M. A. Vinton, W. D. Lauenroth, M. R. Aguiar, D. A. Wedin, R. A. Virginia, and P. N. Lowe (2002), Regional analysis of litter quality in the central grassland region of North America, *J. Veg. Sci.*, *13*, 395–402.

Mutanga, O., and A. K. Skidmore (2004), Predicting in situ pasture quality in the Kruger National Park, South Africa, using continuum-removed absorption features, *Remote Sens. Environ.*, *89*, 393–408.

Parton, W. J., et al. (1995), Impact of climate change on grassland production and soil carbon worldwide, *Global Change Biol.*, *1*, 13–22.

Pastor, J., M. A. Stillwell, and D. Tilman (1987), Little bluestem litter dynamics in Minnesota old fields, *Oecologia*, *72*, 327–330.

Schimel, D. S., W. J. Parton, T. G. F. Kittel, D. S. Ojima, and C. V. Cole (1990), Grassland biogeochemistry: Links to atmospheric processes, *Clim. Change*, *17*, 13–25.

Schimel, D. S., B. H. Braswell, R. McKeown, D. S. Ojima, W. J. Parton, and W. Pulliam (1996), Climate and nitrogen controls on the geography and timescales of terrestrial biogeochemical cycling, *Global Biogeochem. Cycles*, *10*, 677–692.

Schimel, D. S., B. H. Braswell, and W. J. Parton (1997), Equilibration of the terrestrial water, nitrogen, and carbon cycles, *Proc. Natl. Acad. Sci. U. S. A.*, *94*, 8280–8283.

Spanner, M. A., D. L. Peterson, W. Acevedo, and P. Matson (1985), High-resolution spectrometry of leaf and canopy chemistry for biogeochemical cycling, paper presented at Airborne Imaging Spectrometer Data Analysis Workshop, Jet Propul. Lab., Pasadena, Calif.

Streck, N. A., D. Rundquist, and J. Connet (2002), Estimating residual wheat dry matter from remote sensing, *Photogramm. Eng. Remote Sens.*, *68*, 1193–1201.

Throop, H. L., E. A. Holland, W. J. Parton, D. S. Ojima, and C. A. Keough (2004), Effects of nitrogen deposition and insect herbivory on patterns of ecosystem-level carbon and nitrogen dynamics: Results from the CENTURY model, *Global Change Biol.*, *10*, 1092–1105.

Tieszen, L. L., B. C. Reed, N. B. Bliss, B. K. Wylie, and D. D. DeJong (1997), NDVI, C3 and C4 production, and distributions in Great Plains grassland land cover classes, *Ecol. Appl.*, *7*, 59–78.

Waring, R. H., J. D. Aber, J. M. Melillo, and B. I. Moore (1986), Precursors of change in terrestrial ecosystems, *Bioscience*, *36*, 433–438.

Wessman, C. A., J. D. Aber, D. L. Peterson, and J. M. Melillo (1988), Remote sensing of canopy chemistry and nitrogen cycling in temperate forest ecosystem, *Nature*, *335*, 154–156.

White, M. A., P. E. Thornton, S. W. Running, and R. R. Nemani (2000), Parameterization and sensitivity analysis of the BIOME-BGC terrestrial ecosystem model: Net primary production controls, *Earth Interact.*, *4*, 1–85.

Wright, I. J., et al. (2004), Assessing the generality of global leaf trait relationships, *New Phytol.*, *166*, 485–496.

O. Beeri, University of North Dakota Center for People and the Environment, Box 9007, Grand Forks, ND 58202, USA.

M. Liebig and R. L. Phillips, Northern Great Plains Research Laboratory, USDA-ARS, Highway 6 South, P.O. Box 459, Mandan, ND 58554, USA. (phillips@mandan.ars.usda.gov)